

## **Thermal Wave Resonator: *In Situ* Investigation by Photothermal Deflection Technique<sup>1</sup>**

**M. Bertolotti,<sup>2,3</sup> G. L. Liakhou,<sup>4</sup> R. Li Voti,<sup>2</sup> S. Paoloni,<sup>2</sup> and C. Sibilìa<sup>2</sup>**

---

The photothermal deflection technique applied to a gas thermal wave resonator seems to be one of the most powerful techniques to investigate *in situ* the thermal diffusivity of the gas. After a brief description of what a thermal wave resonator really is, a discussion is presented of the advantages and disadvantages of its use for measuring the gas thermal diffusivity.

---

**KEY WORDS:** air; interference; photothermal deflection technique; thermal diffusivity; thermal wave.

### **1. INTRODUCTION**

Although thermal wave interferometry [1] has been applied for a long time to measure the thickness or the thermal diffusivity of thin solids, the name thermal-wave resonator [2] was introduced just 2 years ago. Basically the physical process which takes place in a thin film periodically heated on one side is absolutely the same as that which occurs in a thermal wave resonant cavity: the behavior may be described using the interference between thermal waves propagating in opposite directions.

A plane thermal wave resonator is an open cavity between two solid samples with plane facets which behave as mirrors. From a thermal point of view this condition is practically always verified. In fact due to the great differences between the thermal effusivities of solids and gases, when a thermal wave propagating in the gas approaches the solid, the temperature rise

---

<sup>1</sup> Paper presented at the Thirteenth Symposium on Thermophysical Properties, June 22–27, 1997, Boulder, Colorado, U.S.A.

<sup>2</sup> Dipartimento di Energetica, Università di Roma “La Sapienza”, and GNEQP of CNR and INFN, Via Scarpa 16, 00161, Roma, Italy.

<sup>3</sup> To whom correspondence should be addressed.

<sup>4</sup> Technical University of Moldova, Stefan Cel Mare 168, 277012, Kishinau, Moldova, Italy.

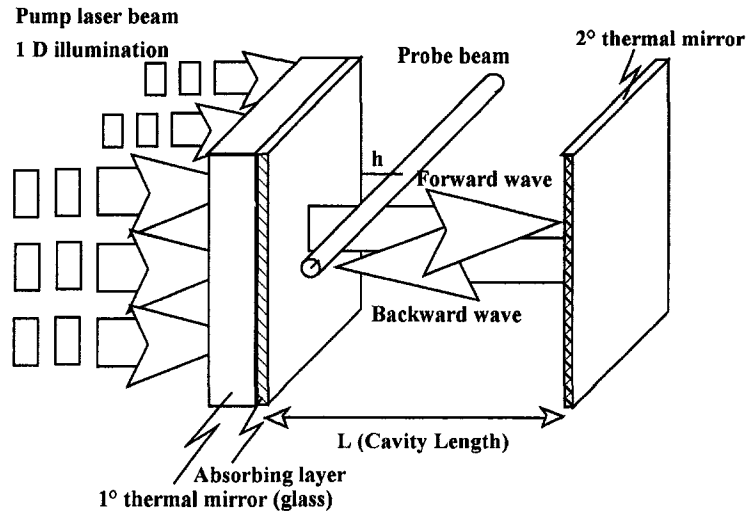


Fig. 1. Schematic representation of a thermal-wave resonator cavity; *in situ* investigation by the photothermal deflection technique.

in the solid is zero because the solid has a large *thermal inertia*, but the thermal gradient reaches its maximum value. So if one measures close to the mirror not the temperature rise, but a quantity proportional to the thermal gradient (heat flux, photothermal deflection angle), one finds a double value that means an amplification of the signal. So the first use of a resonant cavity (see Fig. 1) is for amplifying a signal related to a thermal flux, as happens, for example, in the photothermal deflection technique for direct measurement of the gas thermal diffusivity.

## 2. MEASUREMENT OF GAS THERMAL DIFFUSIVITY

Generally in order to measure the thermal diffusivity of nonabsorbing gases through the photothermal technique, one has to heat a reference solid sample, in contact with the gas, and look at the heat diffusion induced in the gas itself. One of the simplest methods consists of illuminating the sample periodically by means of a wide spot laser beam (pump) to generate a plane thermal wave in the gas. The oscillating gas temperature depends on the distance from the sample surface  $z$  as follows:

$$T(z, t) \approx \frac{I}{e_s \sqrt{2\pi f}} \exp(-z/l_{\text{gas}}) \cos[2\pi ft - (z/l_{\text{gas}})] \quad (1)$$

where  $I$  is the laser intensity,  $f$  is the modulation frequency,  $l_{\text{gas}} = \sqrt{D_{\text{gas}}/\pi f}$  is the gas thermal diffusion length, and  $D_{\text{gas}}$  is the gas thermal diffusivity, while  $e_s$  is the sample thermal effusivity. To detect it, a second laser beam (probe) can be used traveling in the gas at some distance  $z$  from the solid. Its deflection induced by the thermal gradient in  $z$  (mirage effect) is given by

$$\Phi = \frac{l_{\text{path}}}{n_{\text{gas}}} \left( \frac{dn_{\text{gas}}}{dT} \right) \frac{dT(z)}{dz} \quad (2)$$

where  $n_{\text{gas}}$  and  $dn_{\text{gas}}/dT$  are the refractive index and the optothermal coefficient of the gas, respectively and  $l_{\text{path}}$  is the effective length in which the probe beam deflection occurs. By combining Eq. (2) with Eq. (1) and looking at  $\Phi$  in terms of amplitude and phase, one can write

$$\begin{aligned} \ln(|\Phi|) &= (-z/l_{\text{gas}}) + \ln \left( \frac{l_{\text{path}}}{n_{\text{gas}}} \frac{dn_{\text{gas}}}{dT} \frac{I}{k_s} \sqrt{\frac{D_s}{D_{\text{gas}}}} \right) \\ \arg(\Phi) &= (-z/l_{\text{gas}}) + \theta_0 \end{aligned} \quad (3)$$

where  $k_s$  and  $D_s$  are the sample thermal conductivity and diffusivity, while  $\theta_0$  is a constant. Equation (3) shows that both the logarithm of the amplitude and the phase have the same linear behavior as a function of  $z/l_{\text{gas}}$  and suggests two methods to calculate the gas thermal diffusivity.

### 2.1. Frequency scan method

In this method the probe beam travels at a fixed height  $z$ , while the frequency of the periodical heating is changed. By plotting the phase and the logarithm of the amplitude of the photothermal deflection signal as a function of  $\sqrt{f}$ , the same slope is obtained, from which the diffusivity can be determined from one of the two relationships,

$$D_{\text{gas}} = \pi z^2 \left( N_f \left/ \frac{\Delta \ln(|\Phi|)}{\Delta \sqrt{f}} \right. \right)^2 \quad (4a)$$

$$D_{\text{gas}} = \pi z^2 \left( N_f \left/ \frac{\Delta \arg(\Phi)}{\Delta \sqrt{f}} \right. \right)^2 \quad (4b)$$

Note that a corrective factor  $N_f$  has been introduced to take into account the effect of the finite spot size  $a$  of the Gaussian pump beam on the sample surface. The main consequence of a finite spot size is the bending of the plane thermal wave, which, leaving the sample surface, tends gradually to

a spherical wave. In Fig. 2 the result of a numerical study on the factor  $N_f$  is shown. The  $N_f$  values for both amplitude [see Eq. (4a)] and phase [see Eq. (4b)] are plotted as a function of the parameter  $a/z$  for different diffusivity ratios  $D_{\text{gas}}/D_s$  (0.2, 0.5, 5). For large values of  $a/z$  all curves tend to the value 1, which represents the value obtained in the case of a plane thermal wave. Note also that  $N_f$  for the phase stays around 1 for any value of  $a/z$ , while  $N_f$  for the amplitude may deviate more from 1. In practice, by choosing a ratio  $a/z$  around 10 and looking at the expression obtained considering the phase, one does not commit a serious error by using  $N_f = 1$  in Eq. (4b). Indeed the main sources of error for  $D_{\text{gas}}$  in this method are due to the inaccuracy of  $z$  and of the calculated slope  $\Delta \arg(\Phi)/\Delta \sqrt{f}$ . Particular care, in fact, should be given to align the probe beam (this means keeping  $z$  constant along the path) and to reduce its spot (this means keeping  $\Delta z$  as low as possible).

## 2.2. Height Scan Method

In this case the frequency (which is related to the thermal wavelength) is fixed, while the probe beam skims the sample surface at different heights  $z$ .

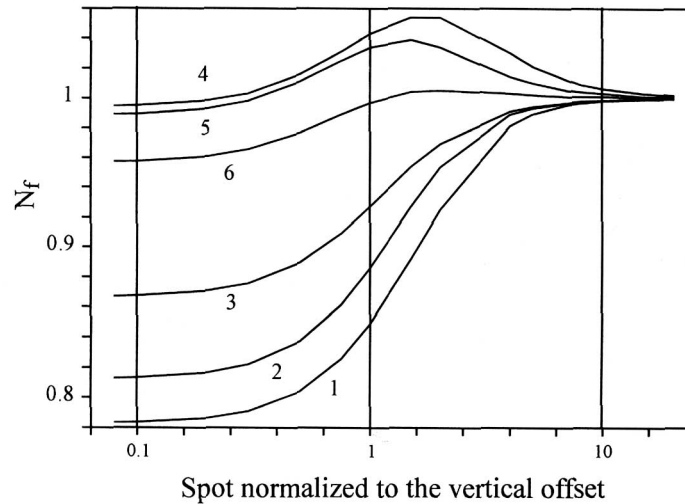


**Fig. 2.** Numerical analysis of the factor  $N_f$  due to the finite spot size of the pump beam. The abscissa is  $a/z$ . The curves refer to different formulae (phase and amplitude) and to different thermal diffusivity ratios between the gas and the sample  $D$ : amplitude formula; (curve 1)  $D = 0.2$ ; (curve 2)  $D = 0.5$ ; (curve 3)  $D = 5$ ; phase formula; (curve 4)  $D = 0.2$ ; (curve 5)  $D = 0.5$ ; (curve 6)  $D = 5$ .

By plotting the data on the phase and the logarithm of the amplitude as a function of  $z$ , the same slopes are obtained, from which the diffusivity can be determined from the two relationships,

$$D_{\text{gas}} = \pi f \left( N_z \left/ \frac{\Delta \ln(|\Phi|)}{\Delta z} \right. \right)^2 \quad (5a)$$

$$D_{\text{gas}} = \pi f \left( N_z \left/ \frac{\Delta \arg(\Phi)}{\Delta z} \right. \right)^2 \quad (5b)$$

In this case another corrective factor,  $N_z$ , has been introduced to take into account the effect of  $a$ . In Fig. 3 the results of a numerical study on the factor  $N_z$  are shown. The  $N_z$  values for both amplitude [see Eq. (5a)] and phase [see Eq. (5b)] are plotted for different diffusivity ratios  $D_{\text{gas}}/D_s$  (0.2, 0.5, 5) as a function of the parameter  $a/l_{\text{gas}}$ , which remains constant during the measurement. Also, in this case, it turns out that the larger  $a/l_{\text{gas}}$  is, the more all curves tend to the value of 1 and that, only for the phase,  $N_z$  is kept around 1 for any value of  $a/l_{\text{gas}}$  and diffusivity. The suggestion is therefore to apply Eq. (5b) without considering the influence of  $N_z$  (this means making  $N_z = 1$ ). Note that in this case the absolute value of  $z$  is not used and the accuracy of Eq. (5b) is better than that of Eq. (4b).

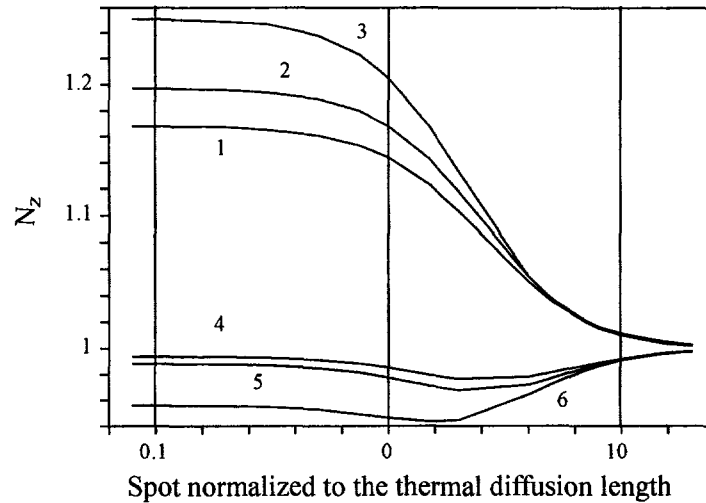


Fig. 3. Numerical analysis of the factor  $N_z$  due to the finite spot size of the pump beam. The abscissa is  $a/l_{\text{gas}}$ . The curves refer to different formulae (phase and amplitude) and to different thermal diffusivity ratios between the gas and the sample  $D$ : amplitude formula; (curve 1)  $D = 0.2$ ; (curve 2)  $D = 0.5$ ; (curve 3)  $D = 5$ ; phase formula; (curve 4)  $D = 0.2$ ; (curve 5)  $D = 0.5$ ; (curve 6)  $D = 5$ .

### 3. THERMAL DIFFUSIVITY MEASUREMENT IN A THERMAL CAVITY

Another approach for measuring the gas thermal diffusivity refers to the study of the deflection angle inside a gas thermal wave resonator. In this case the simple thermal wave resonator shown in Fig. 1 is used. It is made of two plane thermal mirrors and is filled with the gas to be measured. The first plane mirror is a thick glass layer coated with a thin pump-absorbing film (1- $\mu\text{m}$  silicon). On one hand the use of glass allows the reflection of the thermal waves inside the cavity, and on the other hand, it lets the pump beam, coming from outside the cavity, directly illuminate the thin film. The second plane mirror is a thin aluminium foil (20  $\mu\text{m}$ ). It is noteworthy that this thickness is larger than that needed to behave as a thermal mirror [3].

The probe beam is placed inside the cavity at a distance  $z$  from the first mirror, which is also the heat source. The theory of thermal wave interferometry applied to this simple system allows one to write for the deflection angle,

$$\Phi = \left( \frac{l_{\text{path}}}{n_{\text{gas}}} \frac{dn_{\text{gas}}}{dT} \frac{I}{k_s} \sqrt{\frac{D_s}{D_{\text{gas}}}} \right) \times \frac{\exp[-(1+j)z/l_{\text{gas}}] + R_2 \exp[-(1+j)(2L-z)/l_{\text{gas}}]}{1 - R_1 R_2 \exp[-2(1+j)L/l_{\text{gas}}]} \quad (6)$$

where  $L$  is the cavity length, and  $R_1$  and  $R_2$  are the thermal wave reflectivities of the two mirrors, usually ranging between 0.99 and 1. By comparing the deflection in the cavity [Eq. (6)] with the deflection with no cavity [Eq. (3) or, more simply, Eq. (6) with the second mirror removed,  $R_2 = 0$ ], one immediately realizes that the cavity behaves as a deflection amplifier, which, theoretically, in the case of a thin cavity ( $z, L \ll l_{\text{gas}}$ ) has a gain  $(1 + R_2)/(1 - R_1 R_2)$  that is a large quantity considering that  $R_1$  and  $R_2 \cong 1$ . In practice, the gain decreases when one considers the effect of the finite pump spot size  $a$ . In fact, the heating, in this case, produces plane thermal waves propagating not only along the cavity but also in undesired directions, resulting in a loss of amplification. Although Eq. (6) guarantees a stronger signal, the amplitude and phase signal have a complex behavior so that no easy way seems to exist, except a nonlinear fit, for calculating the gas thermal diffusivity.

A different method is thus considered, obtained by an alternative way of looking at Eq. (6). The deflection, in fact, can be seen as the sum of two terms which refer to the forward and backward thermal waves. It is well-known that the ratio between the backward and the forward waves, that is,

the *reflection coefficient*, has an easy single-exponential expression useful for a linear fit. One may therefore ask if it is possible, starting from the sum of the two quantities in Eq. (6), to calculate their ratio. The answer is positive, if additional information is provided, as, for example, the value of the forward wave when the backward wave is absent. In other words, to calculate the reflection coefficient  $\Gamma$  the deflection  $\Phi$  has to be compared with its value with no cavity or when the cavity length  $L$  is infinite. The coefficient  $\Gamma$  is then given by [4]

$$\Gamma(L) = \frac{\Phi(L) - \Phi(\infty)}{\Phi(L) + \Phi(\infty)} = \frac{R_2(1 + R_1)}{2} \exp[-2(1 + j)(L - z)/l_{\text{gas}}]$$

so that

$$\begin{aligned} \ln(|\Gamma|) &= -2(L - z)/l_{\text{gas}} + \ln[R_2(1 + R_1)/2] \\ \arg(\Gamma) &= -2(L - z)/l_{\text{gas}} \end{aligned} \quad (7)$$

Note that both the logarithm of the amplitude and the phase of the reflection coefficient have the same linear behavior in the three variables,  $L$ ,  $z$ , and  $\sqrt{f}$ . The introduction of a new degree of freedom increases the number of methods useful for thermal diffusivity measurements. However, the method we want to describe consists of calculating the reflection coefficient as a function of the cavity length  $L$ , which can be varied by moving only the second mirror ( $z$  and  $\sqrt{f}$  are constant). Using the linear slopes of either the phase or the logarithm of the amplitude of  $\Gamma$  the diffusivity can be determined from one of the two relationships,

$$D_{\text{gas}} = 4\pi f (N_L / [\Delta \ln(|\Gamma|) / \Delta L])^2 \quad (8a)$$

$$D_{\text{gas}} = 4\pi f (N_L / [\Delta \arg(\Gamma) / \Delta L])^2 \quad (8b)$$

As usual, the corrective factor  $N_L$  has been introduced to consider the effect of  $a$ . In Fig. 4 the result of a numerical study on the factor  $N_L$  is presented. The  $N_L$  values for both amplitude [see Eq. (8a)] and phase [see Eq. (8b)] are plotted for different diffusivity ratios  $D_{\text{gas}}/D_s$  (0.2, 0.5, 5) as a function of the parameter  $a/l_{\text{gas}}$ , which remains constant during the measurement. For large  $a/l_{\text{gas}}$ , all the curves tend to 1, but in different ways, such that the amplitude formula in Eq. (8a) is preferred for  $a/l_{\text{gas}} > 2$ .

From a comparison of the three methods we have discussed, we can conclude that there are similarities among the different formulae for  $D_{\text{gas}}$  [see Eqs. (4), (5), and (8)]; in fact, in all cases, they are given by the product of three terms: the slope of the experimental data versus the

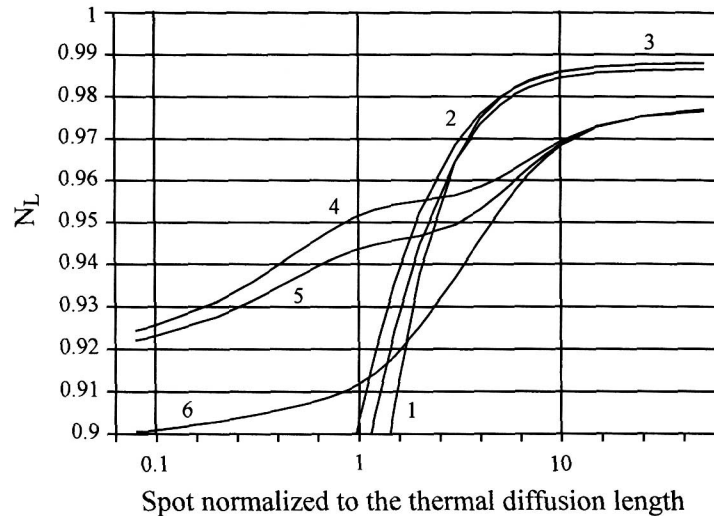


**Fig. 4.** Numerical analysis of the factor  $N_L$ , due to the finite spot size of the pump beam. The abscissa is  $a/l_{\text{gas}}$ . The curves refer to different formulae (phase and amplitude) and to different thermal diffusivity ratios between the gas and the sample  $D$ : amplitude formula; (curve 1)  $D = 0.2$ ; (curve 2)  $D = 0.5$ ; (curve 3)  $D = 5$ ; phase formula; (curve 4)  $D = 0.2$ ; (curve 5)  $D = 0.5$ ; (curve 6)  $D = 5$ .

variable chosen for the scan; the other variable, which is kept constant; and a corrective factor  $N$ . Concerning the accuracy, the spatial scan methods, as discussed above, give better results compared to the frequency scan methods. Finally, the use of a thermal wave resonator does not improve the corrective factor ( $N_z$  and  $N_L$  tend to 1 in a similar way), but due to the deflection gain, the accuracy of the experimental data, and hence of the calculated slope, is strongly increased. In the case of a gas with non-homogeneous diffusivity, it is noted that each method can give, depending on the methodology on which it is based, different aspects of the gas thermal diffusivity. In fact, the first method provides an effective local diffusivity measurement, the second gives rise to the average diffusivity from the sample to the probe beam, while the third, by using the interference in the cavity, measures the average diffusivity in the whole resonator.

#### 4. RESULTS

The cavity length scan method has been applied to measure the air thermal diffusivity inside the plane open resonator in Fig. 1. The scan has been performed by moving the second mirror, a 20- $\mu\text{m}$ -thick aluminium foil, to vary the cavity length  $L$  from 100 to more than 1300  $\mu\text{m}$ . The probe



beam has been placed at about  $70\ \mu\text{m}$  from the first mirror, the silicon-coated glass sample, which has been illuminated by a 250-mW Ar laser with a spot on the silicon film of about 1 mm. A mechanical chopper frequency of  $f = 36\ \text{Hz}$  was selected to have  $a/l_{\text{gas}} \cong 2.3$ .

The photothermal signal should be normalized to the reference signal that corresponds to an infinite cavity length. In practice, one can use as a reference the photothermal signal for the maximum cavity length of  $1300\ \mu\text{m}$ . This distance inhibits the thermal waves from doing a complete round-trip in the resonator. In Fig. 5 both the phase and the natural logarithm of the amplitude are plotted versus the cavity length. Looking at the logarithm of the amplitude one may note that within the first  $300\ \mu\text{m}$  (just one-half of the air diffusion length), there is a gain in the deflection signal which reaches its maximum value of 11 dB. The reason for this low gain is due to radial losses. By applying Eq. (7), the reflection coefficient  $\Gamma$  is determined. In Fig. 6 both the phase and the natural logarithm of the amplitude of  $\Gamma$  are plotted versus the cavity length  $L$ . The expected linear behavior is observed over the first  $500\ \mu\text{m}$ , until the interference between the damped forward and backward waves becomes ineffective. Looking at the linear slopes and using Eq. (8), one can calculate the air thermal diffusivity. In this case, a small distortion from linearity occurs for both the phase and the logarithm of the amplitude. This effect can be related to the variable value of the air diffusivity. In fact with 250 mW of pump beam

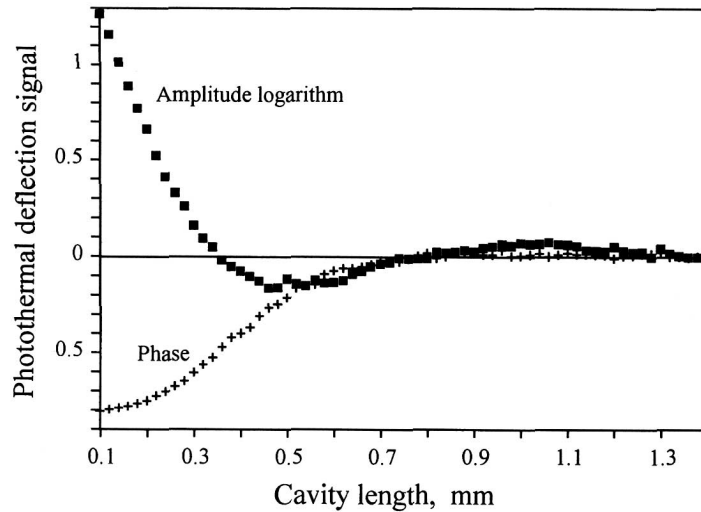


Fig. 5. Phase (radian) and natural logarithm of amplitude of the deflection signal as a function of cavity length  $L$  (mm). The frequency is fixed at  $f = 36\ \text{Hz}$ . The spot size is 1 mm. The thermal wave resonator works in air.

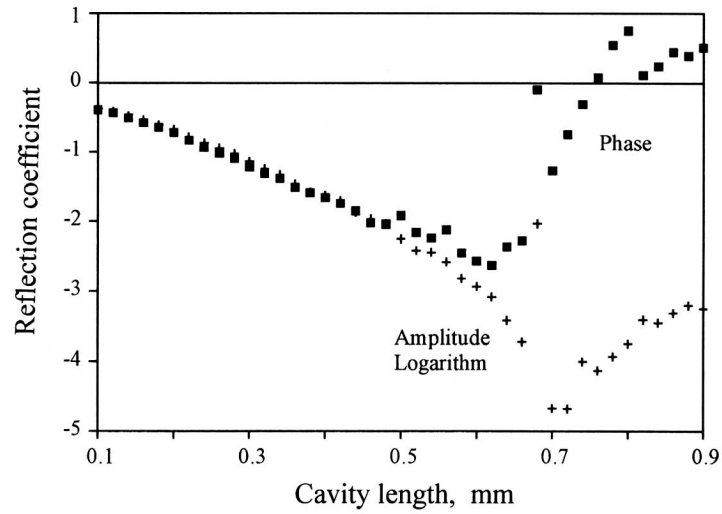


Fig. 6. Phase (radian) and natural logarithm of amplitude for the reflection coefficient  $\Gamma$  as a function of cavity length  $L$  (mm). The data were obtained using Eq. (7).

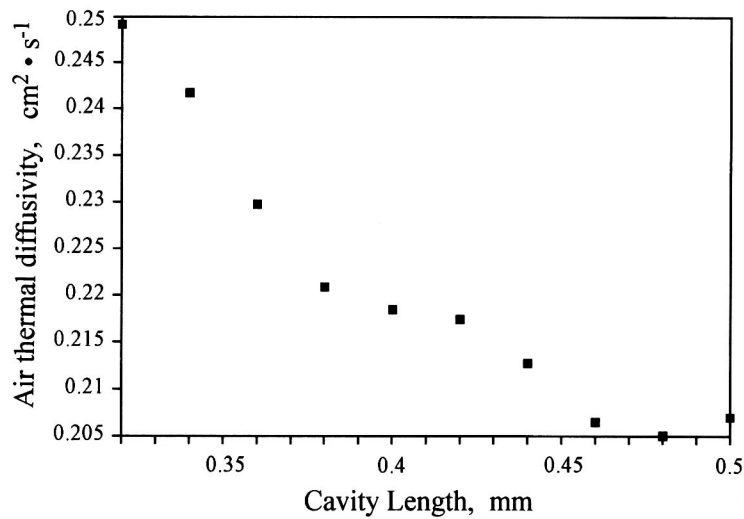


Fig. 7. Air thermal diffusivity measurements vs cavity length  $L$  (mm).

power, by changing the cavity length of the resonator, the DC temperature rise inside could change by several tens of degrees, which could to increase the air thermal diffusivity by several percent. By applying Eq. (8) locally, one obtains the calculated profile of the air thermal diffusivity as a function of the cavity length (see Fig. 7). For cavity lengths larger than  $450\ \mu\text{m}$ , the effect of the DC temperature rise becomes negligible such that the diffusivity levels to the standard value of  $0.21\ \text{cm}^2 \cdot \text{s}^{-1}$  at a room temperature of  $20^\circ\text{C}$  [5].

## 5. CONCLUSIONS

The theory of the plane thermal wave resonator is introduced for a gas cavity. The use of such a device to perform accurate gas thermal diffusivity measurement is demonstrated. Finally, the experimental results on an air thermal resonator confirm the theory and give an example of how to calculate the air thermal diffusivity profile.

## REFERENCES

1. C. A. Bennett Jr. and R. R. Patty, *Appl. Opt.* **21**:49 (1982).
2. J. Shen and A. Mandelis, *Rev. Sci. Instrum.* **66**:4999 (1995).
3. M. Bertolotti, R. Li Voti, C. Sibilìa, and G. L. Liakhov, *SPIE* **2775**:370 (1996).
4. M. Bertolotti, M. Firpo, R. Li Voti, S. Paoloni, C. Sibilìa, F. Tani, and G. L. Liakhov, *Prog. Nat. Sci.* **6**:219 (1996).
5. Y. S. Touloukian, R. W. Powell, C. Y. Yo, and M. C. Nicolaou, in *Thermophysical Properties of Matter, Vol. 10. Thermal Diffusivity* (Plenum, New York, 1973).